ELEC ENG 3BB3:

Cellular Bioelectricity

Notes for Lecture 15

Thursday, February 6, 2014

Propagation velocity constraint for uniform (unmyelinated) fiber:

For uniform propagation, the space-time behaviour of $V_m(x,t)$ must satisfy the wave equation:

$$V_m(x,t) = V_m\left(t - \frac{x}{\theta}\right), \qquad (6.64)$$

where θ is the *propagation velocity* and the waveform for V_m on the RHS is the temporal waveform, i.e., $V_m(t)$.

Propagation velocity constraint for uniform (unmyelinated) fiber:

Alternatively:

$$V_m(x,t) = V_m(x - \theta t)\,, \qquad (6.64')$$

where the waveform for V_m on the RHS is the spatial waveform, i.e., $V_m(x)$.

(Note that propagation of the action potential waveform without dissipation requires an active membrane, i.e., voltage-gated ion channels.)

Propagation velocity constraint for uniform (unmyelinated) fiber (cont.):

Differentiating Eqn. (6.64) once with respect to x, utilizing the chain rule, gives:

$$\frac{\partial V_m}{\partial x} = -(1/\theta)\frac{\partial V_m}{\partial t}, \qquad (6.65)$$

and again results in:

$$\frac{\partial^2 V_m}{\partial x^2} = \left(1/\theta^2\right)\frac{\partial^2 V_m}{\partial t^2}. \qquad (6.66)$$

Propagation velocity constraint for uniform (unmyelinated) fiber (cont.):

Substituting Eqn. (6.66) into (6.31), with $i_p = 0$, $r_e = 0$ & $r_i = R_i/\pi a^2$, gives:

$$\frac{a}{2R_i\theta^2}\frac{\mathrm{d}^2V_m}{\mathrm{d}t^2} = C_m\frac{\mathrm{d}V_m}{\mathrm{d}t} + g_{\mathrm{K}}(V_m - E_{\mathrm{K}}) + g_{\mathrm{Na}}(V_m - E_{\mathrm{Na}}) + g_L(V_m - E_L) \qquad (6.68)$$

With an appropriate value for θ the solution to this ODE exhibits an action potential; the solution diverges with an incorrect θ.

Propagation velocity constraint for uniform (unmyelinated) fiber (cont.):

An important property of the propagation velocity can be obtained with inspection of Eqn. (6.68) without solving it explicitly.

Note that all the terms on the right-hand side (6.68) are independent of the fiber radius a, as is d^2V_m/dt^2, and thus the coefficient must be a constant independent of a, that is:

$$\frac{a}{2R_i\theta^2} = \text{constant} = \frac{1}{K}. \qquad (6.69)$$

Propagation velocity constraint for uniform (unmyelinated) fiber (cont.):

Consequently:

$$\theta = \sqrt{\frac{aK}{2R_i}} \, . \qquad (6.70)$$

Since K is unknown, it must be determined experimentally.

An empirically-obtained relationship for squid giant axon at 18.3°C is:

$$\theta = \sqrt{d} \quad \text{m/s}, \qquad (6.71)$$

where d is the fiber diameter in μm.

Propagation in myelinated nerve fibers:

In vertebrates, Schwann cells produce myelin which wraps around an axon to produce an insulating sheath. The regularly-space breaks in the myelin are called *nodes of Ranvier*, and the axon segments between nodes are referred to as *internodes*.

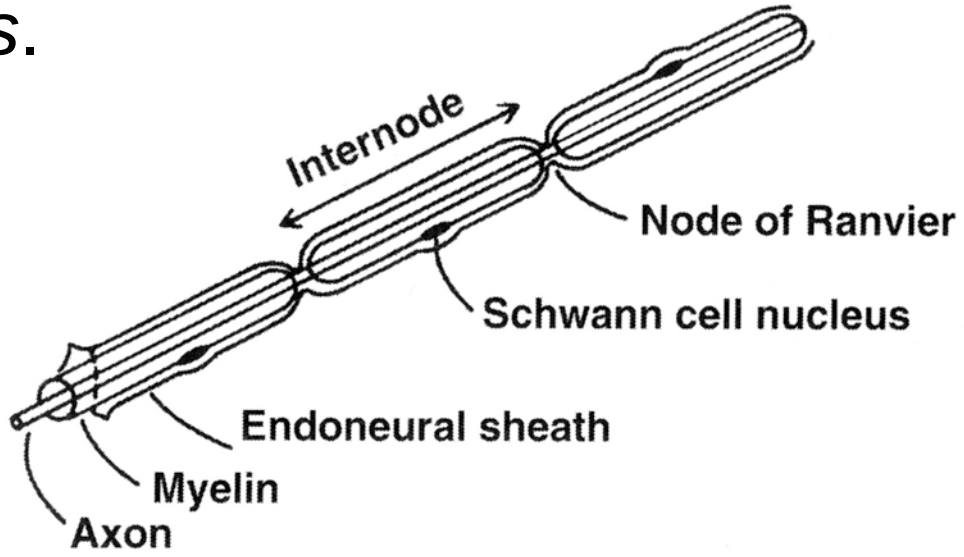

Figure 6.11. Diagram Showing the Structure of a Myelinated Nerve Fiber. Reprinted with permission from Aidley DJ. 1978. *The physiology of excitable cells*. Cambridge: Cambridge UP.

Propagation in myelinated nerve fibers (cont.):

The myelin is wrapped in layers around the axon, often on the order of 10s or even 100s of layers.

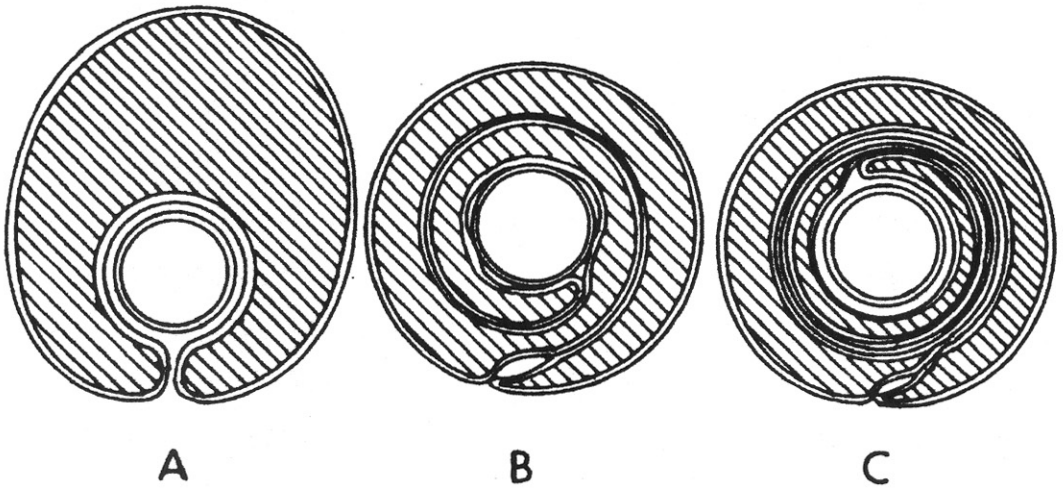

Figure 6.12. The Development of the Myelin Sheath by Vertebrate Schwann Cells in the Sequence. $A \rightarrow B \rightarrow C$. Reprinted with permission from Robertson JV. 1960. The molecular structure and contact relationships of the cell membrane. *Prog Biophys* **10**:343–417. Copyright ©1960, Pergamon Journals Ltd.

Propagation in myelinated nerve fibers (cont.):

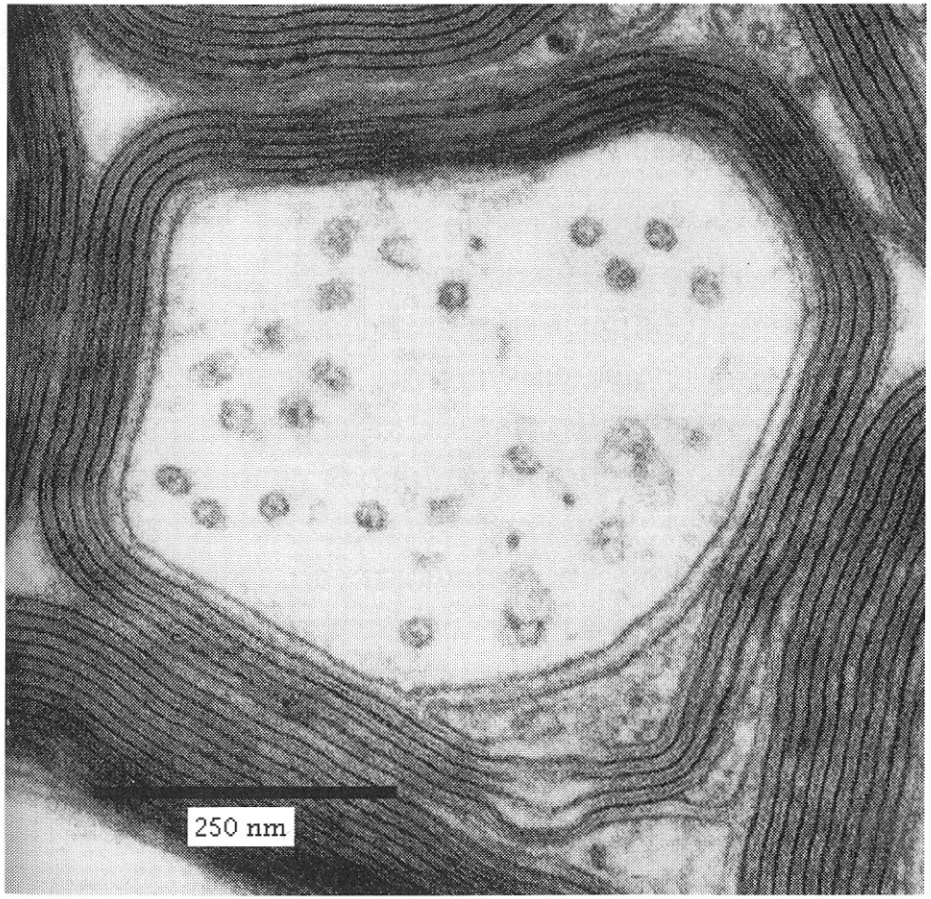

Fig. 6.14 MYELINATED AXONS Electron micrograph of a cross section through a portion of the optic fiber in an adult rat. The complete transverse section through a single myelinated axon is shown in close neighborhood to other axons. About four wrappings of myelin insulation are visible. The circular structures inside the axonal cytoplasm are transverse sections through microtubules. Reprinted by permission from Peters, Palay, and Webster (1976).

(from Koch)

Propagation in myelinated nerve fibers (cont.):

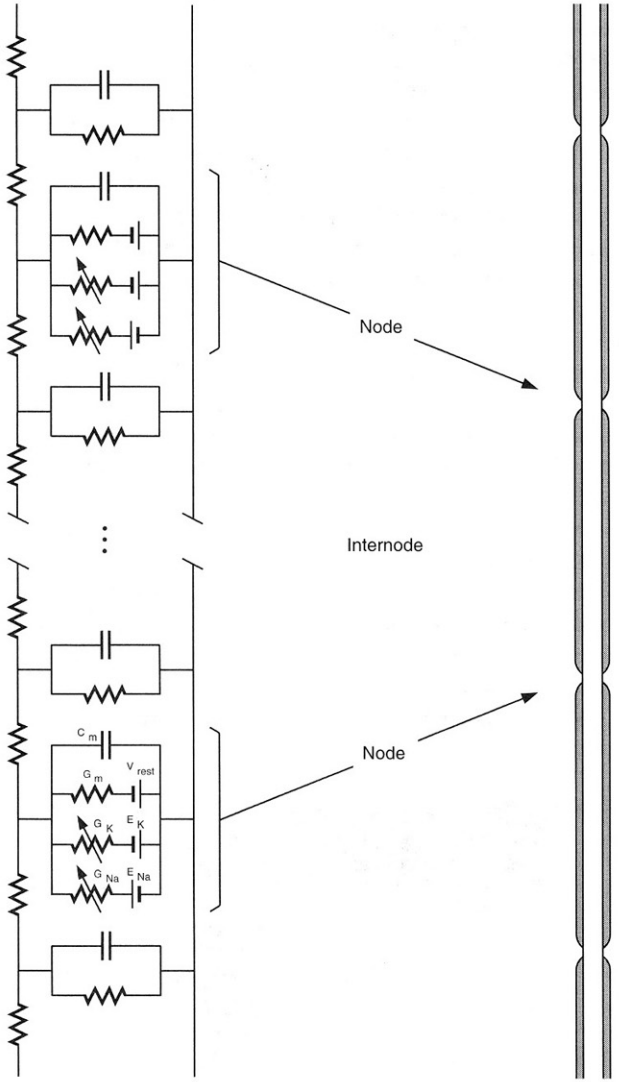

Fig. 6.15 Electrical Circuit for a Myelinated Axon Geometrical and electrical layout of the myelinated axon from the frog sciatic nerve (Frankenhaeuser and Huxley, 1964; Rogart and Ritchie, 1977). The diameter of the axon and its myelin sheath is 15 μm, the diameter of the axon itself 10.5 μm, the difference being made up by 250 wrappings of myelin. The myelin is interrupted every 1.38 mm by a *node of Ranvier* that is 2.5 μm wide. The total distributed capacitance for the internode (2.2 pF) is only slightly larger than the capacitance of the much smaller node (1.6 pF). The same is also true of the distributed resistance. At each node, the spike is reamplified by a fast sodium current and is repolarized by a potassium current. Little or no potassium current is found at the nodes of Ranvier in mammalian myelinated axons. There, repolarization is accomplished by rapid sodium inactivation in conjunction with a large effective "leak" current.

(from Koch)

Propagation in myelinated nerve fibers (cont.):

The specific leakage resistances and specific capacitances of the myelin sheath and cell membrane shown below are consistent with the myelin sheath being equivalent to around 100 layers of cell membrane.

Table 6.2. Electrical Properties of Myelin Sheath and Cell

	Specific leakage resistance (Ω cm^2)	Specific capacitance (F/cm^2)
Myelin sheath	10^5	10^{-8}
Cell membrane	10^3	10^{-6}

Propagation in myelinated nerve fibers (cont.):

Considering the Frankenhaeuser–Huxley model under subthreshold (i.e., linear/passive) conditions, the nodes of Ranvier have a specific membrane resistance and specific membrane capacitance of:

$$R_m = 20\ \Omega\ \mathrm{cm}^2$$

and (6.72)

$$C_m = 3\ \mu\mathrm{F}/\mathrm{cm}^2,$$

respectively.

Propagation in myelinated nerve fibers (cont.):

Note:-

- Nodes of Ranvier are around 1 μm in length.
- Internodal distances are on the order of 1 to 2 mm. (A rough empirical rule is that the internodal length equals 100£ d, where d is the fiber diameter.)

Although internodes are much longer than nodes, the much smaller specific capacitance of the former means that an internode and a node have approximately the same capacitance.

Propagation in myelinated nerve fibers (cont.):

The purpose of the myelin is clearly to:

1. reduce the capacitance of long stretches of membrane, the *internodes*, such that they are more easily charged up as an AP propagates through, and
2. increase the membrane leakage resistance so that there is less leakage across the membrane of the intracellular longitudinal current.

Consequently, the “local circuit currents” extend over much longer lengths of the fiber.

Propagation in myelinated nerve fibers (cont.):

Because the local circuit currents extend from one node to the next node (or several nodes ahead in some cases):

1. action potentials propagate faster, and
2. a “failsafe” mechanism may be provided – if one node is blocked, the action potential may be regenerated at the next node along the axon.

Propagation in myelinated nerve fibers (cont.):

In contrast to (6.72), for frog myelinated fibers:

$$\theta = 6d \quad \text{m/s}, \tag{6.73}$$

where d is the fiber diameter in μm.

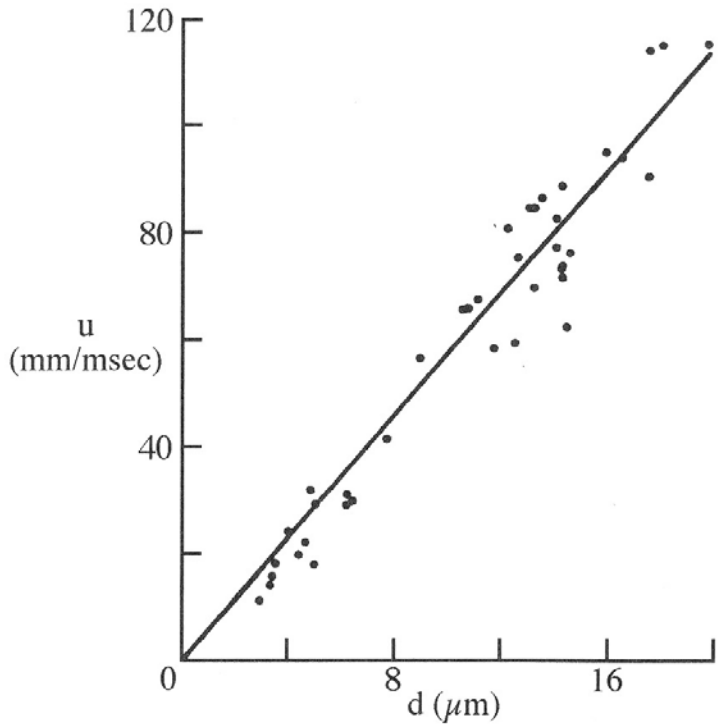

Fig. 6.16 Diameter and Propagation Velocity Relationship between (internal) diameter d of adult cat peripheral myelinated fibers and propagation velocity u of the action potential. The data are shown as dots (Hursh, 1939) and the least-square fit as a line. Peripheral myelinated fibers are bigger than 1 μm, while myelinated fibers in the central nervous system can be as thin as 0.2 μm, with an expected velocity in the 1-mm/msec range. Reprinted by permission from Ritchie (1982).

(from Koch)

Propagation in myelinated nerve fibers (cont.):

Propagation along a myelinated axon has historically been referred to as *saltatory propagation*, as if APs effectively jump or skip from node to node.

This is based on the observations that:

1. the extracellular potential outside an internode does not change much as the AP propagates by, and
2. the voltage-gated sodium channels are concentrated at the nodes of Ranvier.

Propagation in myelinated nerve fibers (cont.):

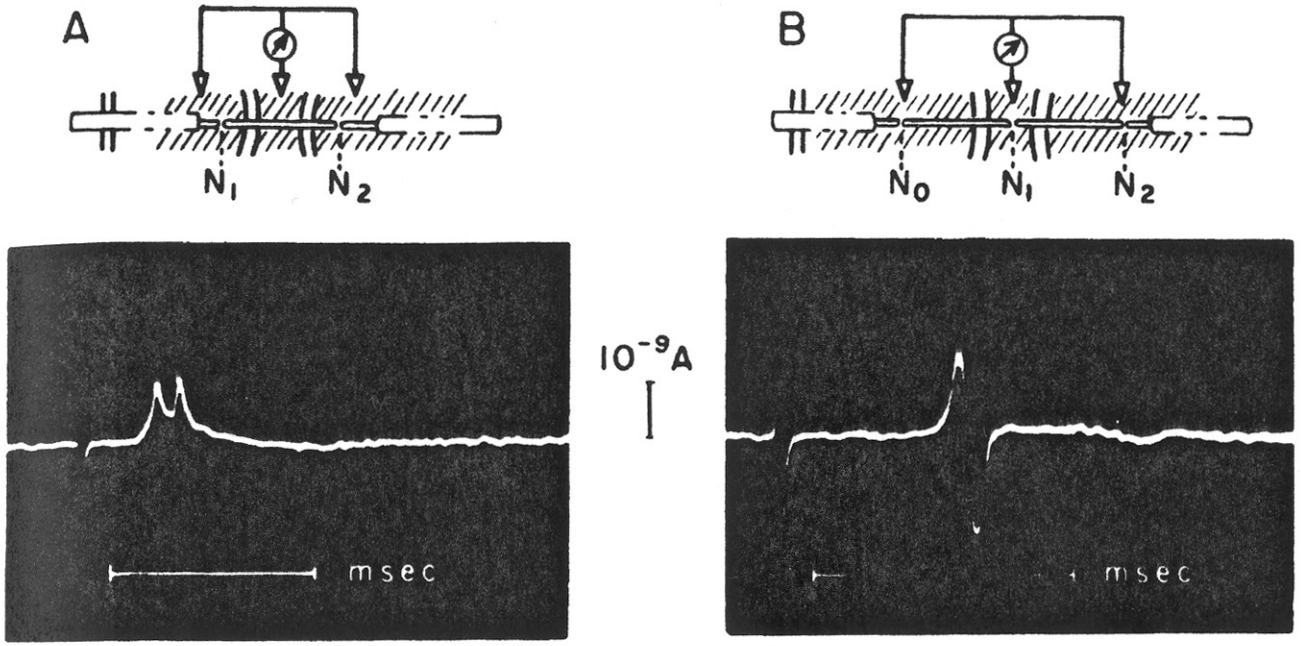

Figure 6.13. The Radial Currents in a short length of a myelinated fiber during the passage of an action potential. The upper part of the Figure describes the recording arrangement and the lower part the recorded currents. (A) The tracing shows the membrane current when the middle pool of Ringer does not contain a node. (B) The membrane current is measured when the middle pool contains a node. Nodes are identified as N_0, N_1, N_2. The three extracellular compartments are insulated from each other by the indicated insulating diaphragm. From Tasaki I, Takeuchi T. 1942. Weitere studien über den aktionsstrom der narkhaltiger nervefaser und über die elektrosaltatorische übertragung des nervenimpulses. *Pflugers Arch Ges Physiol* **245**:764–782.

Propagation in myelinated nerve fibers (cont.):

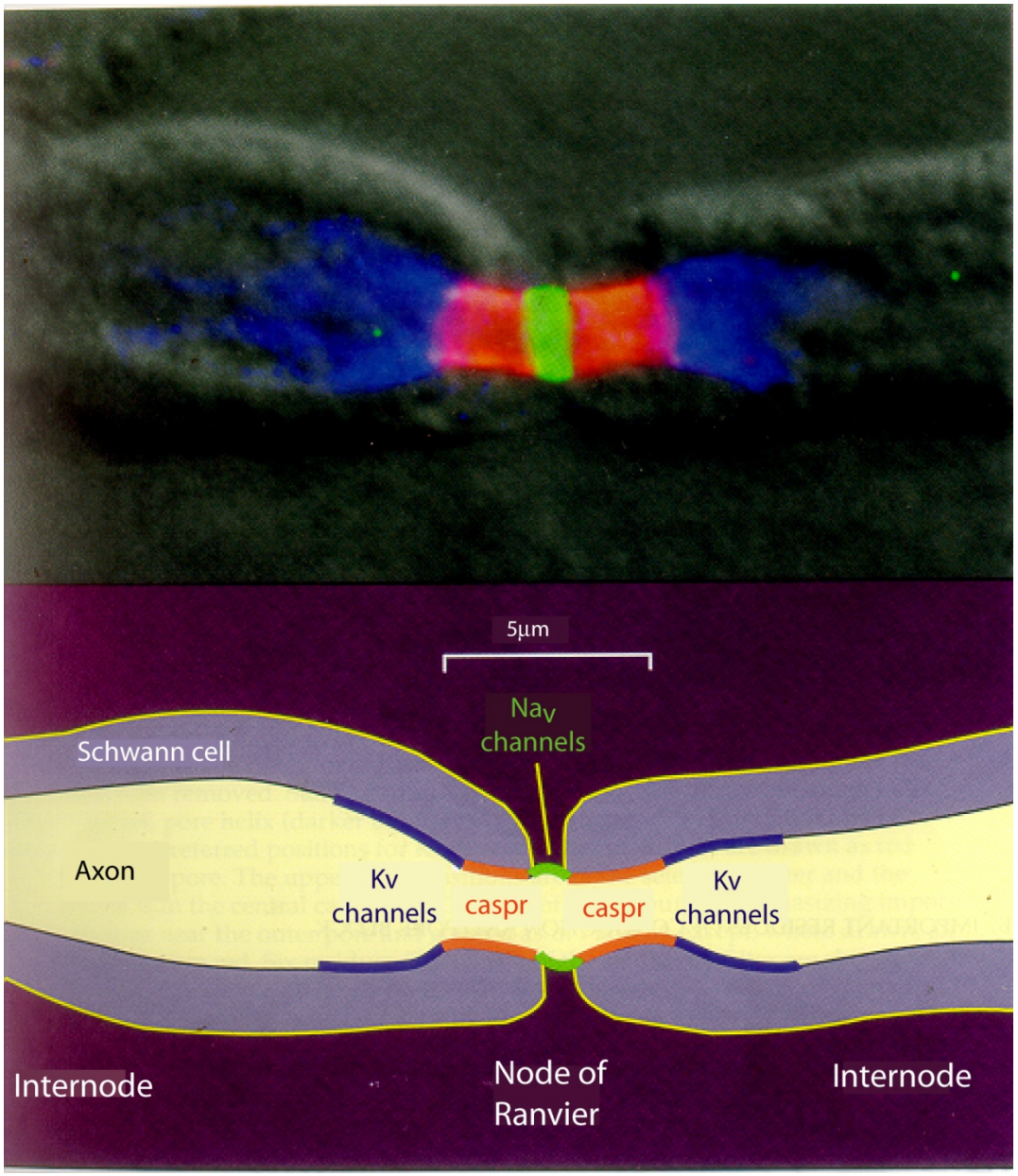

(from Hille)

Propagation in myelinated nerve fibers (cont.):

However, the conductive nature of the axoplasm means that the transmembrane potential along an internode must deviate from rest as the action potential propagates from one node of Ranvier to the next.

In fact, the AP transmembrane potential waveform is attenuated somewhat as it propagates along the internode and then grows again as it approaches the next node.

Additional Gating Information

- The following slides are not req'd but included to show where some research is going

Specialized location of neural ion channels:

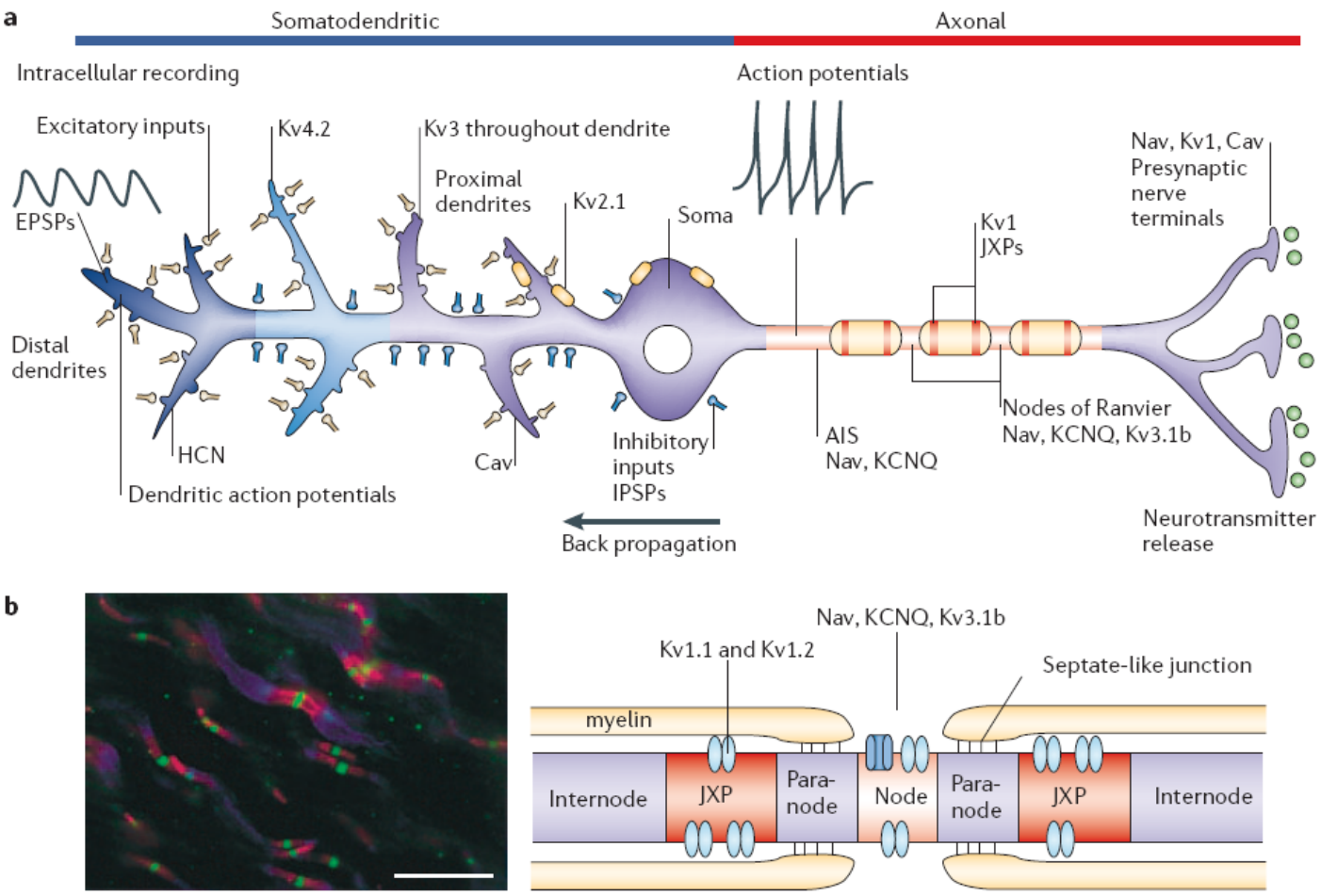

(Lai and Jan, 2006)

Families of ion channels:

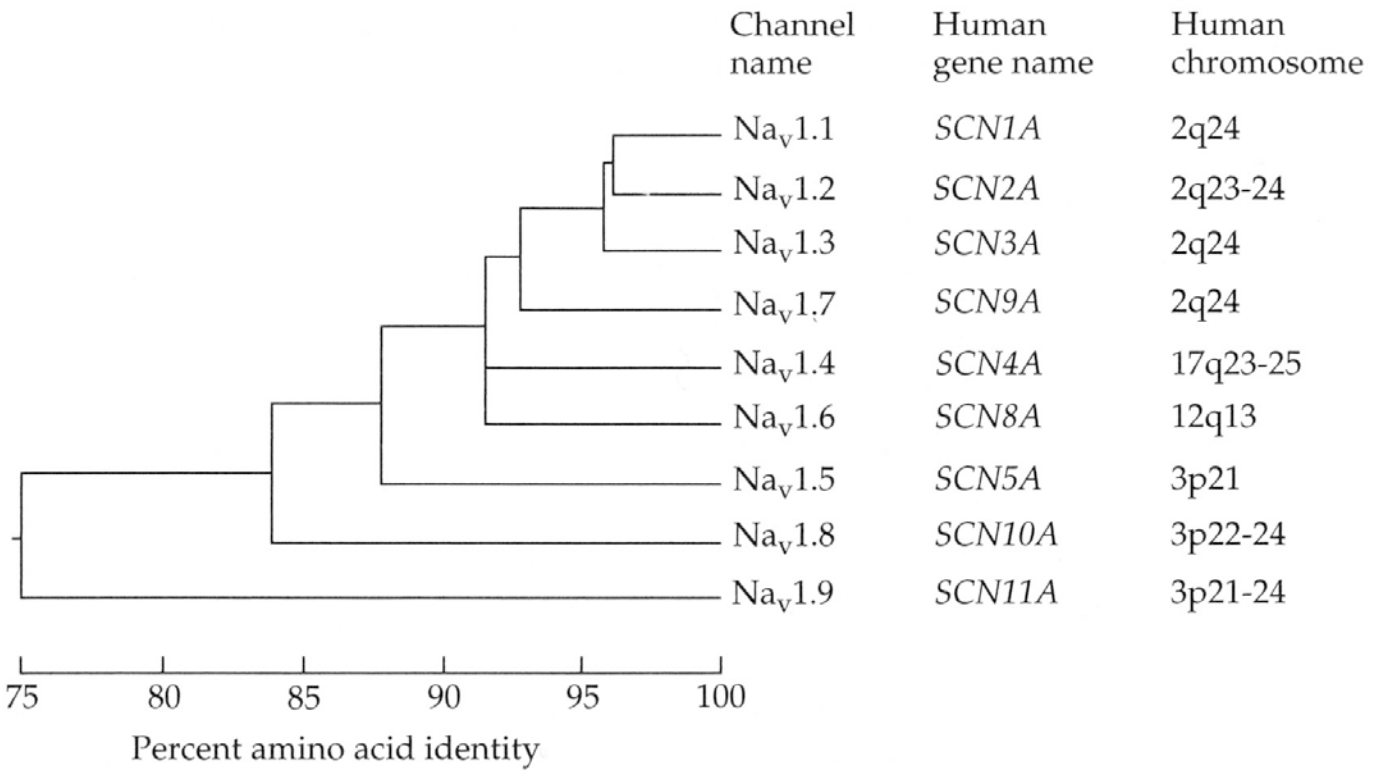

3.13 A Dendrogram of Na Channels Comparison of the amino acid sequences of nine α subunits for expressed mammalian Na channels. Additional related sequences exist but have not been expressed. The more similar the sequences for a pair of genes, the shorter is the path connecting them. Therefore, the diagram may reflect the path of gene duplications in phylogeny. Calculations were made by the Clustal algorithm using a subset of the amino acids comprising the repeat domains I through IV and the III-IV cytoplasmic linker. [From Goldin et al. 2000]

(Hille 2001)

Families of ion channels (cont.):

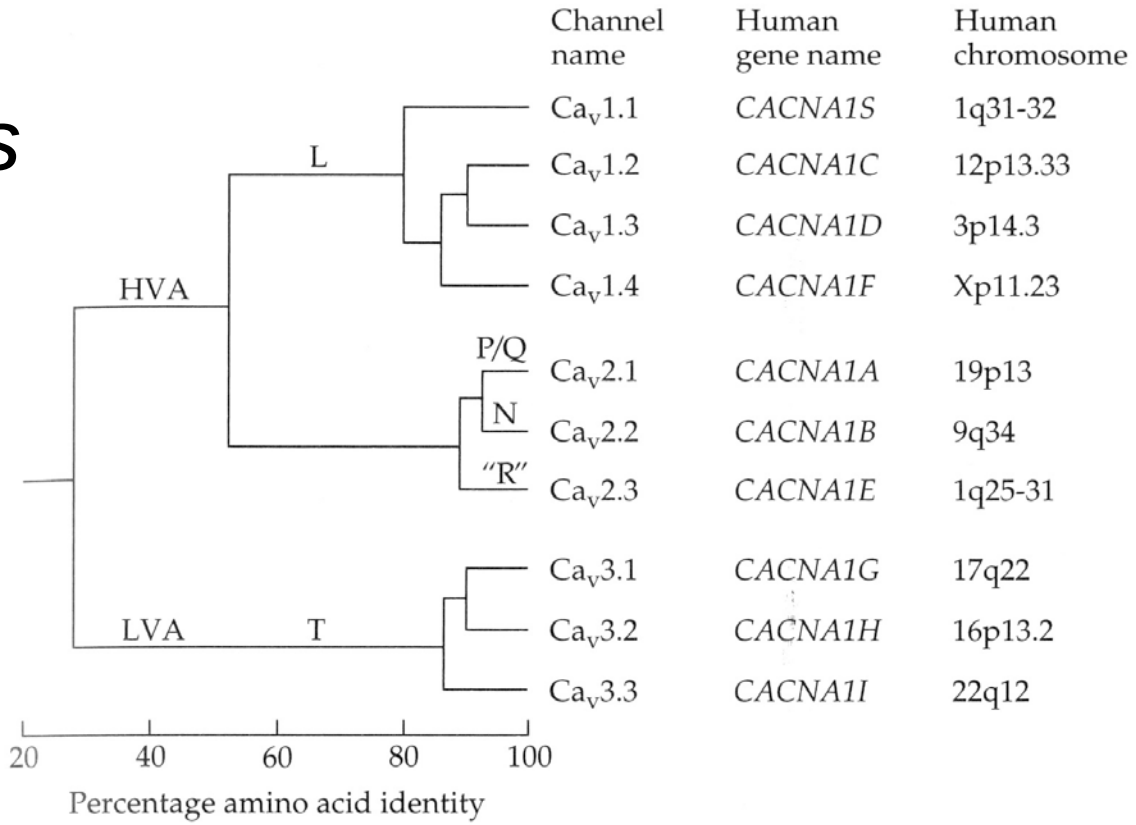

4.16 Three Subfamilies of Ca Channel Genes A dendrogram comparing the amino acid sequences of α_1 subunits of voltage-gated Ca channels using the Clustal algorithm. The comparison was restricted to the six transmembrane segments and the P loops of each homologous repeat domain (about 350 amino acids), so the more divergent intracellular and extracellular loops were not considered. Even in the more conserved regions, the HVA and LVA channel are quite different. The structural nomenclature recognizes three broad gene subfamilies—Ca_v1, Ca_v2, and Ca_v3—with closely related members. The official human gene names for α_1 subunits mimic the extended Snutch nomenclature (see Table 4.1). More genes may be discovered. [From Ertel et al. 2000.]

(Hille 2001)

Families of ion channels (cont.):

TABLE 4.1 Types of Ca Channels in Vertebrates

	Slow, persistent	Fast, inactivating	
	HVA	HVA	LVA
Tsien type[a]	L	P/Q, N, R	T
Snutch gene class[b]	S, C, D, F	A, B, E	G, H, I
Structural nomenclature[c]	$Ca_v1.1$, 1.2, 1.3, 1.4	$Ca_v2.1$, 2.2, 2.3	$Ca_v3.1$, 3.2, 3.3
Activation range[d]	Positive to –30 mV	Positive to –20 mV	Positive to –70 mV
Inactivation range	–60 to –10 mV	–120 to –30 mV	–100 to –60 mV
Inactivation[e]	Very slow ($\tau > 500$ ms)	Partial ($\tau \approx 50$–80 ms)	Complete ($\tau \approx 20$–50 ms)
Deactivation rate[f]	Rapid	Slow	Rapid
Single-channel conductance[g]	25 pS	13 pS	8 pS
Single-channel openings	Continual reopening	Long burst	Brief burst, inactivation
Relative conductance	$Ba^{2+} > Ca^{2+}$	$Ba^{2+} > Ca^{2+}$	$Ba^{2+} = Ca^{2+}$
Divalent block	$Cd^{2+} > Ni^{2+}$	$Cd^{2+} > Ni^{2+}$	$Ni^{2+} > Cd^{2+}$
ω-CTX GVIA block[h]	No	Strong for $Ca_v2.2$	No
Dihydropyridine sensitivity[i]	Sensitive	Resistant	Resistant

Table partially after Tsien et al. (1988) for dorsal root ganglion cells at 21°C, with modifications to accommodate newer work.

[a] Tsien et al. (1988)

[b] Snutch et al. (1990); Birnbaumer et al. (1994)

[c] Ertel et al. (2000)

[d] In 10 mM Ca.

[e] Inactivation rate at 0 mV, 10 mM Ca or 10 mM Ba extracellular, EGTA in cell, 21°C.

[f] Rate of turn-off of tail current at –80 to –50 mV.

[g] Maximum slope conductance in 110 mM Ba.

[h] ω-Conotoxin GVIA from *Conus geographus*.

[i] Enhancement by BAY K 8644 and inhibition by nifedipine.

(Hille 2001)

Families of ion channels (cont.):

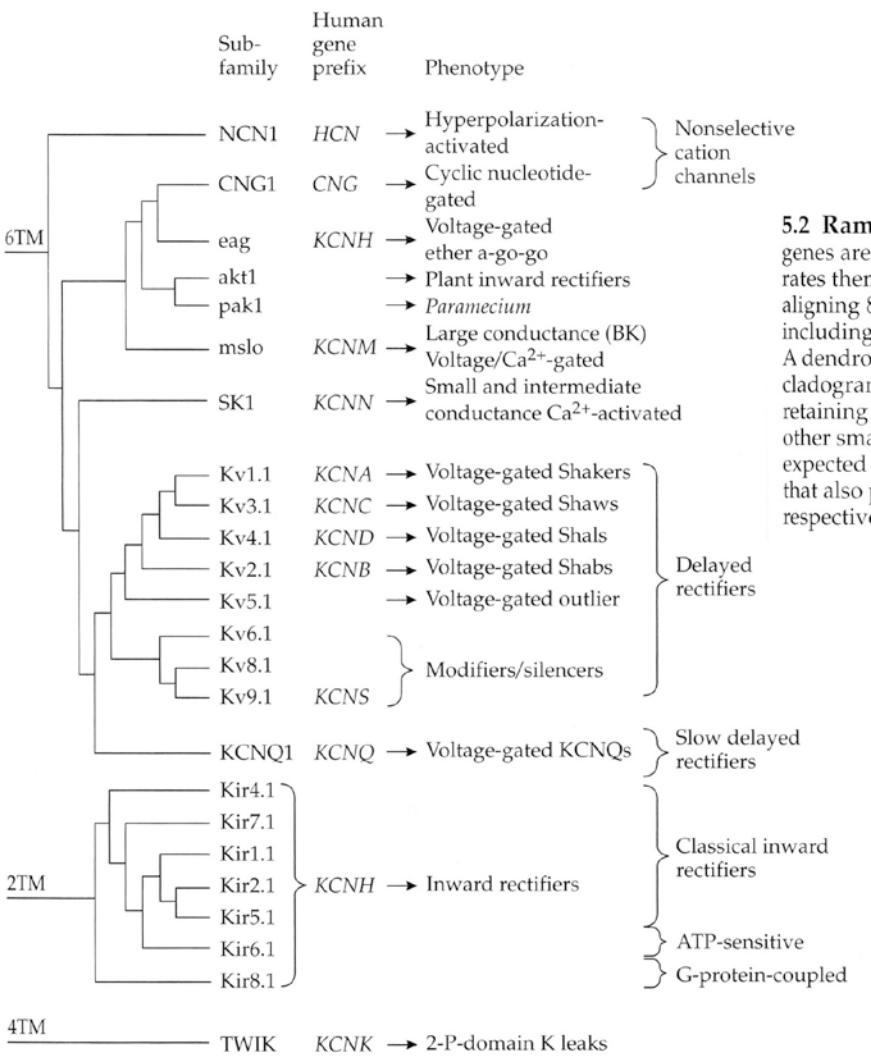

5.2 Ramification of K Channels in Higher Animals Known K-channel genes are sorted by similarity of amino acid sequence. The coarsest grouping separates them by membrane topology (2TM, 4TM, 6TM). This diagram was made by aligning 89 channel sequences, mostly from mammals, using just 47–49 amino acids including their P-regions and extending into the subsequent hydrophobic domain. A dendrogram was made with the Clustal algorithm and then converted into a cladogram using the MacClade program. Finally, the full tree was simplified by retaining only one representative member of each subfamily and discarding the other small branches. Branch lengths do not represent time, but the branching is expected to preserve evolutionary relationships. The HCN channels are relatives that also pass Na^+ ions; the akt and pak channels are from plants and *Paramecium*, respectively. [Kindly prepared by W. J. Joiner and A. M. Quinn.]

(Hille 2001)

Diversity of AP shapes:

(from Koch)

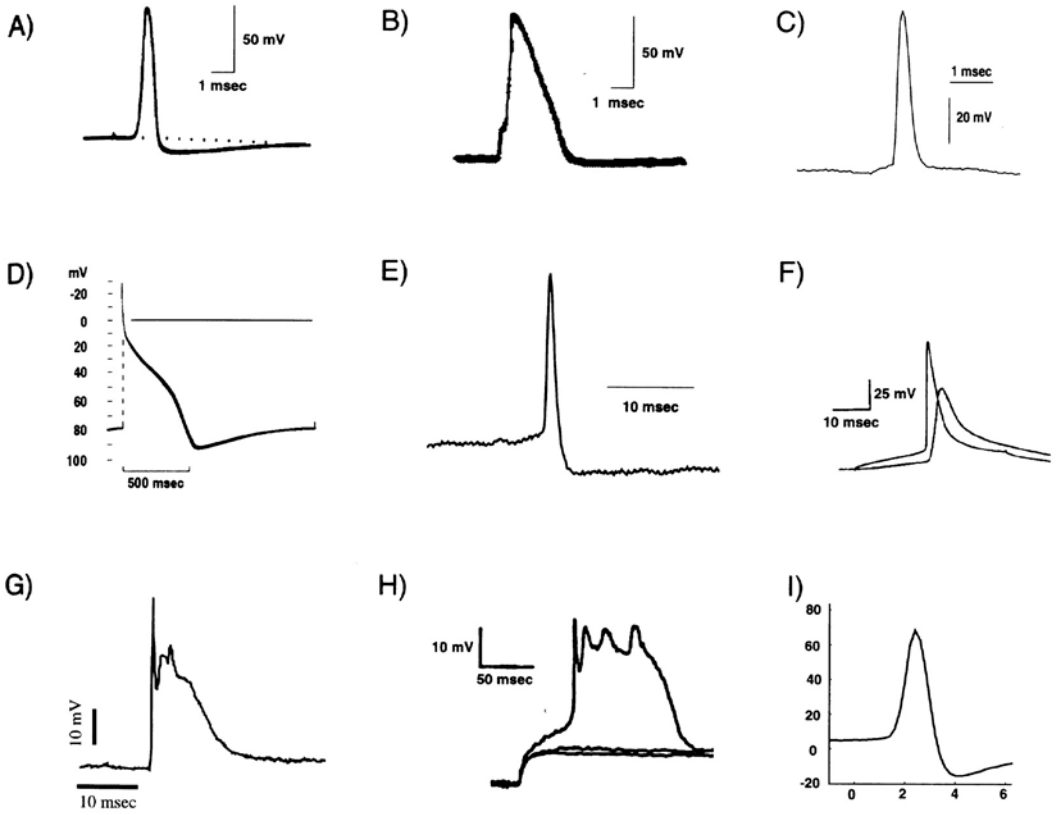

Fig. 6.1 ACTION POTENTIALS OF THE WORLD Action potentials in different invertebrate and vertebrate preparations. Common to all is a threshold below which no impulse is initiated, and a stereotypical shape that depends only on intrinsic membrane properties and not on the type or the duration of the input. **(A)** Giant squid axon at 16° C. Reprinted by permission from Baker, Hodgkin, and Shaw (1962). **(B)** Axonal spike from the node of Ranvier in a myelinated frog fiber at 22° C. Reprinted by permission from Dodge (1963). **(C)** Cat visual cortex at 37° C. Unpublished data from J. Allison, printed with permission. **(D)** Sheep heart Purkinje fiber at 10° C. Reprinted by permission from Weidmann (1956). **(E)** Patch-clamp recording from a rabbit retinal ganglion cell at 37° C. Unpublished data from F. Amthor, printed with permission. **(F)** Layer 5 pyramidal cell in the rat at room temperatures. Simultaneous recordings from the soma and the apical trunk. Reprinted by permission from Stuart and Sakmann (1994). **(G)** A complex spike—consisting of a large EPSP superimposed onto a slow dendritic calcium spike and several fast somatic sodium spikes—from a Purkinje cell body in the rat cerebellum at 36° C. Unpublished data from D. Jaeger, printed with permission. **(H)** Layer 5 pyramidal cell in the rat at room temperature. Three dendritic voltage traces in response to three current steps of different amplitudes reveal the all-or-none character of this slow event. Notice the fast superimposed spikes. Reprinted by permission from Kim and Connors (1993). **(I)** Cell body of a projection neuron in the antennal lobe in the locust at 23° C. Unpublished data from G. Laurent, printed with permission.